

# Summary of Research Activities on Microwave Discharge Phenomena involving Chalmers (Sweden), Institute of Applied Physics (Russia) and CNES (France)

J. Puech<sup>(1)</sup>, D. Anderson<sup>(2)</sup>, M.Lisak<sup>(2)</sup>, E.I. Rakova<sup>(3)</sup>, J. Rasch<sup>(2)</sup>, V. E. Semenov<sup>(3)</sup>, I.A.Shereshevskii<sup>(4)</sup>

<sup>(1)</sup> Centre National d'Etudes Spatiales (Toulouse, France)

<sup>(2)</sup> Chalmers University of Technology (Göteborg, Sweden)

<sup>(3)</sup> Institute of Applied Physics (Nizhny Novgorod, Russia)

<sup>(4)</sup> Institute for Physics of Microstructures, (Nizhny Novgorod, Russia)

## INTRODUCTION

New generation telecommunications satellites are designed to cater for constantly increasing number of users, asking for higher and higher bit rates, in the same frequency multiplex. The combination of these two tendencies implies increasing power levels in the RF equipment downstream from the power amplifiers. In this situation, different types of discharge phenomena can occur inside the microwave devices. The consequences may be link budget degradation or even damage to the equipment. Two kinds of discharges can occur depending on the pressure range:

- in a rarefied atmosphere, an avalanche-like increase of the electron density may occur due to secondary electron emission when electrons, accelerated by the RF electric field, hit the wall of the microwave device ( Multipactor effect)
- at finite pressures, a similar growth of the plasma density in the gas filling the device may occur due to impact ionisation of neutral gas molecules by free electrons ( Corona effect).

A CNES project involving the Institute of Applied Physics (Nizhny Novgorod – Russia), Chalmers University of Technology (Göteborg – Sweden) and Centre National d'Etudes Spatiales (Toulouse – France) is currently investigating a number of aspects in connection with these phenomena. The main goals of the project are first to obtain a good understanding of the physics of the phenomena and then to develop tools capable to predict the power thresholds for both phenomena. The approach chosen is first to create simulation tools for simple cases, to validate them by different algorithms, and then to study more complicated cases (such as complex geometry and/or multi-carrier situations).

## 1. MULTIPACTOR INSIDE CIRCULAR WAVEGUIDES

In standard waveguides (rectangular or circular), a large number of microwave periods is necessary for electrons to cross the distance between the metallic walls. In such waveguides, the microwave electric field is spatially non-uniform. Consequently, the electron trajectories are unstable due to the action of the Miller force (ponderomotive force). These two aspects result in the fact that simulations need tremendous number of electron trajectories and long evolution times. Pure Monte-Carlo algorithm or PIC simulations would require a substantial amount of computational capabilities. A new algorithm has been implemented in order to stay within computation capabilities.

Specifically, a software tool was developed and applied to simulate the Multipactor effect inside circular waveguide, where the fundamental mode  $TE_{11}$  is excited inside the waveguide. Two kinds of polarization were considered in the study: linear and circular polarization. The simulations were completed for the copper waveguide and Fig. 1 presents the simulation results (to the left) as well as a model of the secondary emission yield (SEY) depending on impact electron energy (top the right)

One can notice that, for a given standard circular waveguide, the circular polarization is worse than the linear polarization in term of the risk for Multipactor. But even in the case of the circular polarization, the level of the threshold is quite high, at around 500 – 600 kW.

A more general analysis results in the conclusion that for any given electromagnetic mode and material of the waveguide the Multipactor threshold is determined by the product of the microwave frequency and radius of the waveguide:  $P_{th} = F(\omega R/c)$ , where  $c$  stands for the light velocity in free space. This means that the threshold can be

determined for any standard waveguide. For instance, in a circular copper waveguide with a circular polarization, the threshold is at about 600 kW. The results are not very far away from a standard rectangular waveguide, for which the threshold is at about 200 – 300 kW.

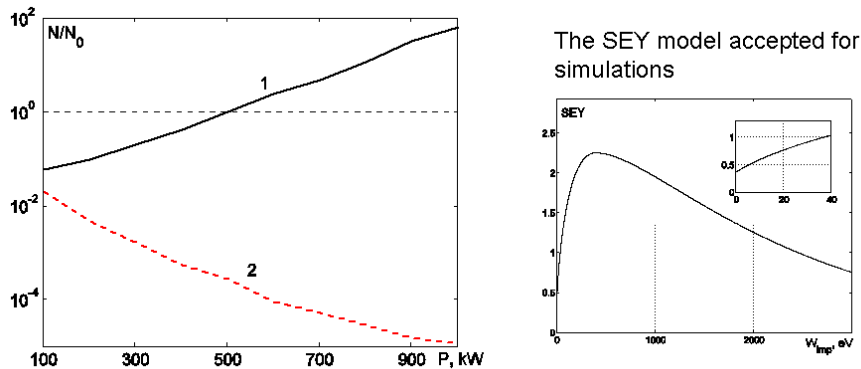


Fig. 1. The relative increase in the number of free electrons ( $N/N_0$ ) inside a circular waveguide depending on the transmitted microwave power,  $P$ . The calculations used a frequency,  $f = 10$  GHz, a waveguide radius,  $R = 1$  cm for circular (curve 1), and linear (curve 2) polarizations. The dependence of the SEY on the impact electron energy,  $W_{imp}$ , is shown on the right panel.

## 2. MULTIPACTOR EFFECT IN A SEPTUM POLARIZER

A septum polarizer is a RF component used mainly inside antenna sub-systems in spacecraft payloads. This 3 port RF component (see Fig. 2) enables the transformation of 2 fundamental rectangular waveguide modes into 2 degenerated modes at the output of the component.

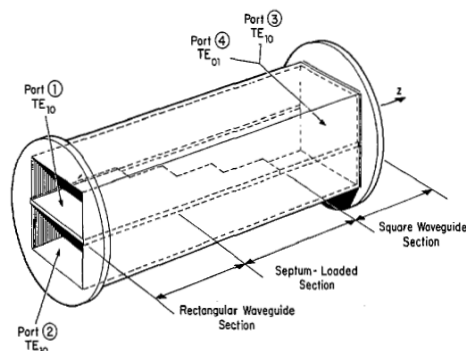


Fig. 2. General view of the septum polarizer.

More specifically, two independent fundamental propagating modes, TE<sub>10</sub>, at the input rectangular waveguides of the polarizers are transformed into 2 degenerated propagating modes at the output square waveguide. Amplitudes and phases are controlled in each of the section of the waveguide so that it is possible to obtain different polarization (circular, linear, elliptic) at the output.

A software tool, “MuPolar”, was developed to simulate the multipactor avalanche inside a separate section of rectangular septum polarizers. MuPolar contains a solver for the electromagnetic field, and a Multipactor simulator based on the Monte-Carlo algorithm.

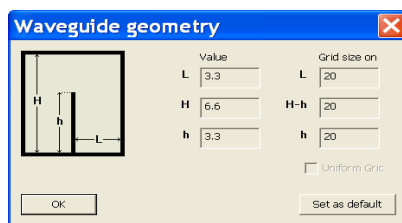


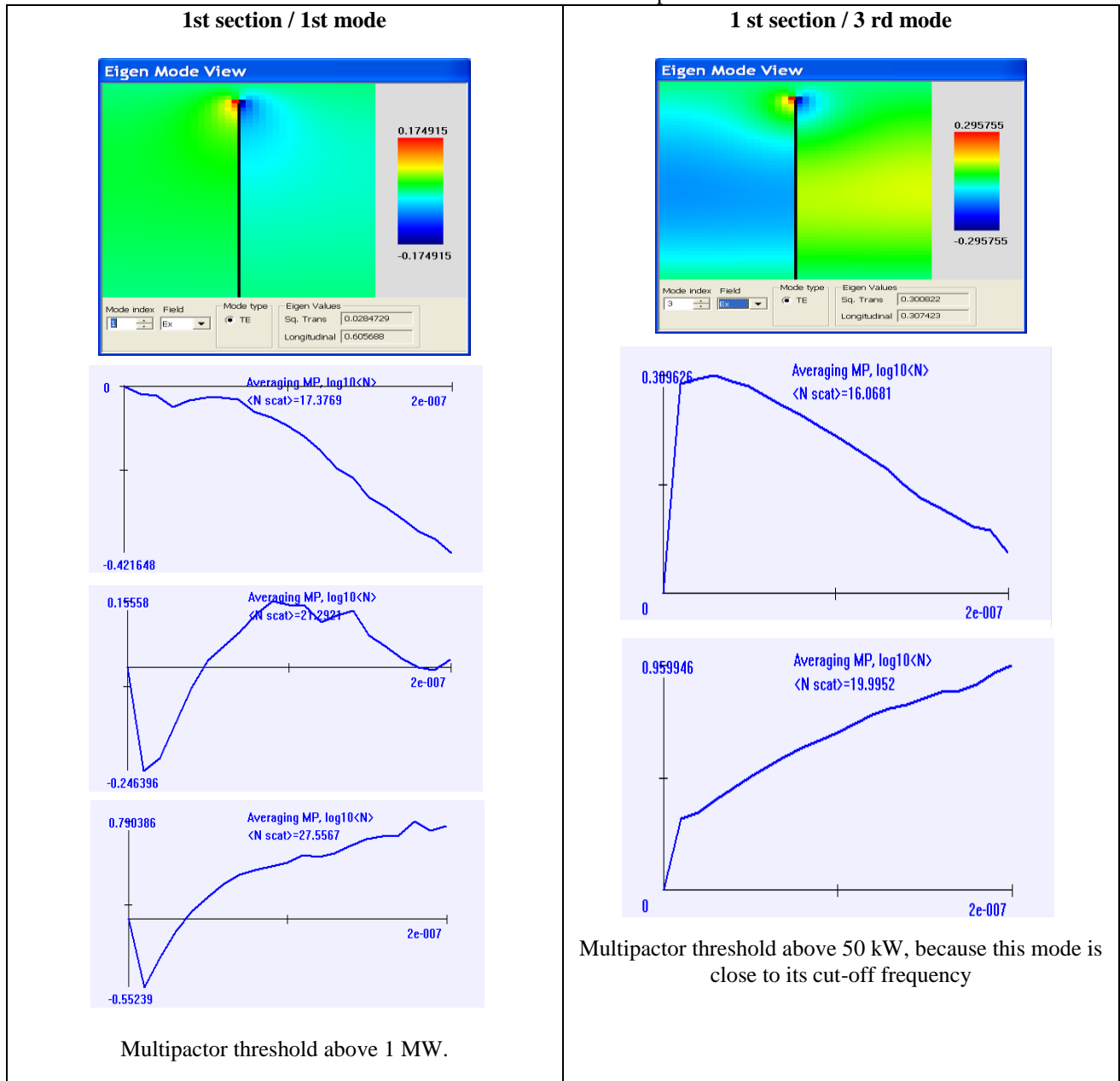
Fig. 3. Parameter specification of the separate transverse cross-section of the polarizer.

The electromagnetic field solver calculates the only propagating TE modes (including their transverse structure and propagation constant) inside rectangular waveguide having a septum normal to bottom wall and placed in the middle of this wall. All geometrical parameters of the system cross section as well as operating frequency can be chosen arbitrarily by the user (see Fig. 3). The software makes it possible to visualize the transverse spatial distribution of all components of the microwave field and the temporal evolution of the relative electron number.

The preliminary simulations were performed using dimensions determined by formulas given in the following article (Chen, IEEE 1973). The septum thickness was taken to be zero. In all these simulations the following set of parameters was used: average initial energy of electrons; 5eV, first cross-over point for the SEY; 30eV, maximum value of SEY; 2.5, number of electron trajectories;  $10^5$ , and duration of the multipactor avalanche; 600 rf periods.

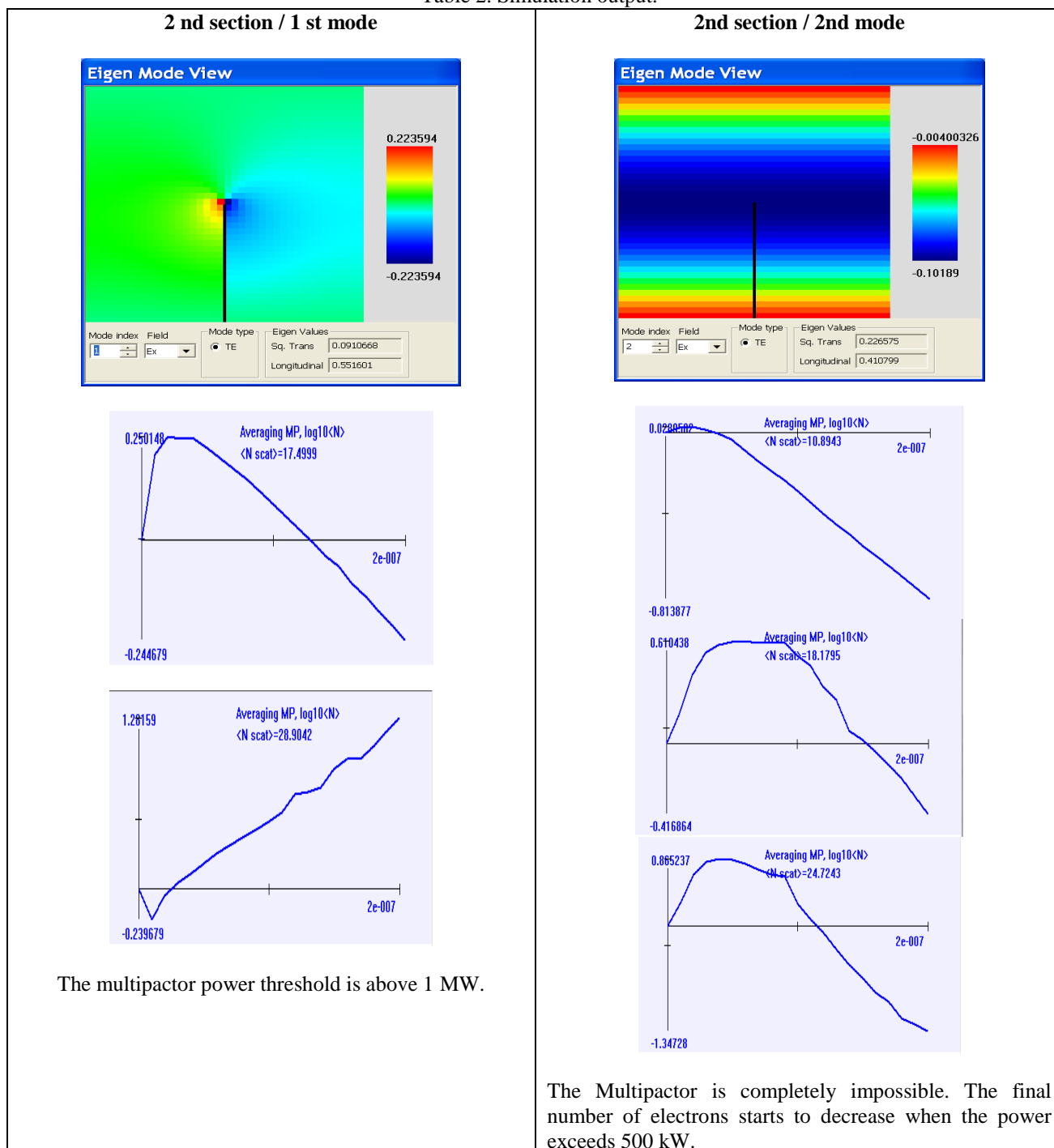
Some simulation results are shown in table 1 and 2 for different sections of the polarizer and different combinations of the modes.

Table 1. Simulation output.



In the second polarizer section the multipactor was simulated also for two different combinations of simultaneous mode excitation. In both combinations the modes transmitted equal power, but were excited with different phase shift (zero or  $\pi/2$ ). In the case of zero phase shift, the total electric field has linear polarization directed preferably along the diagonal of the square waveguide. In the second case (when the modes are excited with the phase shift equal  $\pi/2$ ), the total electric field has preferably circular polarization. In both cases the simulations showed approximately the same power threshold,  $P \approx 600$  kW. In the third and fourth sections it was found that Multipactor can occur only in the case of the first excited mode. The power threshold was found to be about 1 MW and 2.5 MW respectively.

Table 2. Simulation output.



### 3. MULTIPACTOR EFFECT IN THE CASE OF A HALF IRIS

Due to symmetry, the spatial distribution of the rf field inside a half-iris structure coincides completely with that inside half of a complete iris structure. Therefore it is possible to estimate the rate of electron losses which is caused by electron random walk due to initial velocity spread and Miller force effect using the model with finite parallel plates, but taking their effective length  $a_{\text{eff}}=a-(h/2)(2/\pi)$ .

The latter will result in higher level of the multipactor threshold in comparison to the complete iris structure with the same gap width.

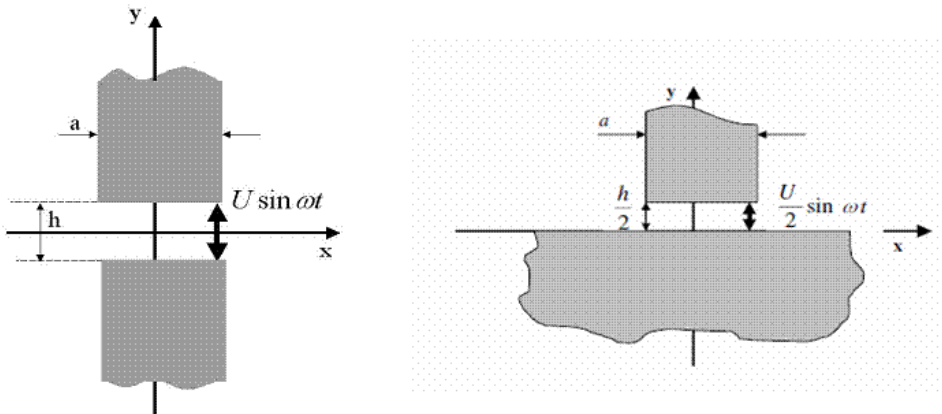


Fig. 4. A comparison between the complete (to the left) and half (to the right) iris structures.

The software Mulsim couples an electromagnetic software based on the Mode Matching technique with a particle trajectories software based on the Monte-Carlo method. It enables the prediction of the Multipactor threshold inside waveguide components. The software Mulsim was upgraded to simulate the Multipactor effect inside the half iris structure. Within the new version of MulSim the user can chose the Vaughan's approximation or adopt any measured set of data for the SEY. The user can also control the starting position of the seed electron which is important in case when the partial standing wave is exited in the section and it is desirable to launch the seed electron close to the rf field maximum when searching for the multipactor threshold.

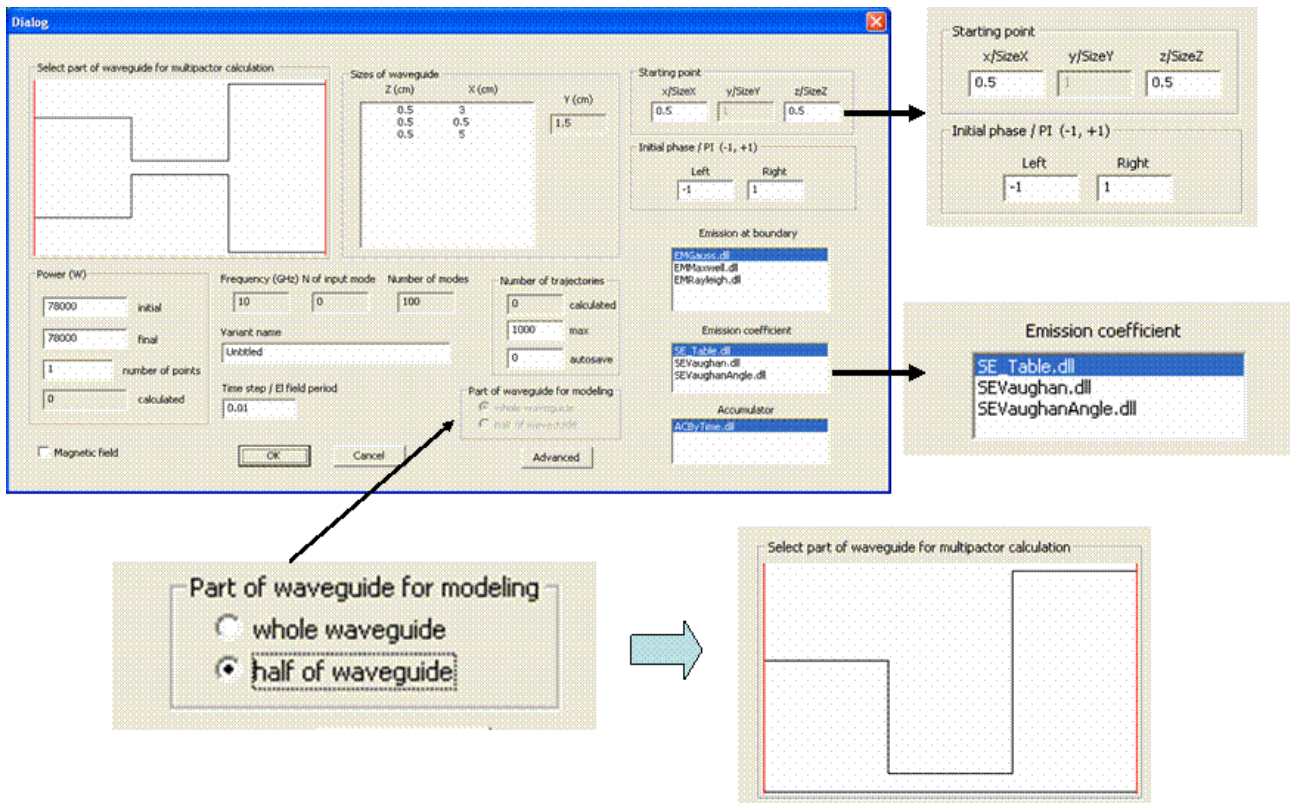


Fig. 5. The main window of MulSim, which allows the user to specify all simulation parameters.

A comparison between the Multipactor simulations inside the complete and half iris structures is illustrated in Figs. 6, 7. On these figures an increase in the relative electron number after 15 rf periods depending on the applied voltage amplitude is shown. The simulation parameters are: maximum SEY=2.22 (within the Vaughan's approximation); the first cross-over point of the secondary emission curve,  $E_1=59$  eV, average initial energy of secondary electrons (within Maxwell probability distribution)  $W_0=4$  eV, frequency,  $f=9.56$  GHz.

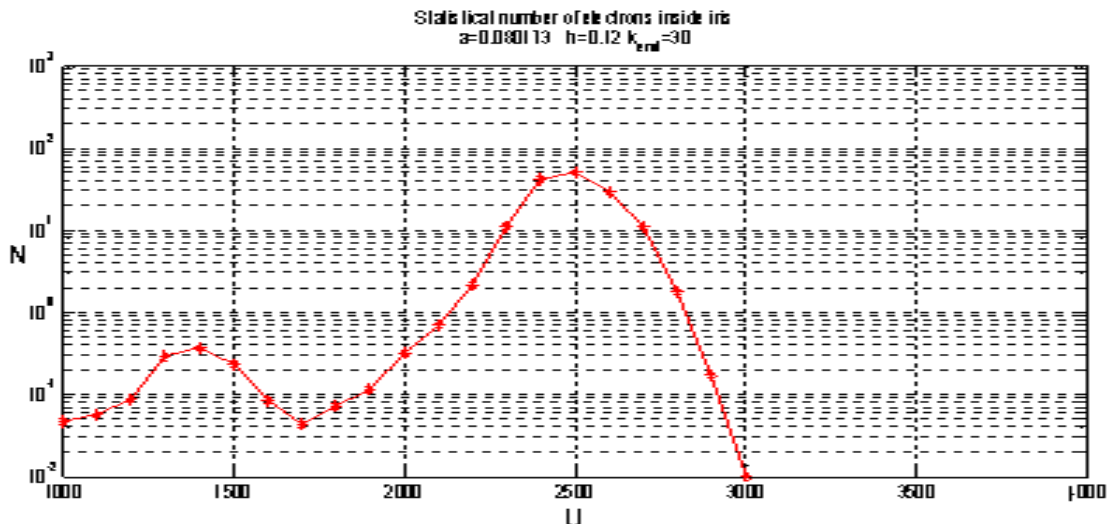


Fig. 6. The relative number of electrons after 15 microwave periods inside the complete iris structure with height 0.12 cm and length 0.08 cm

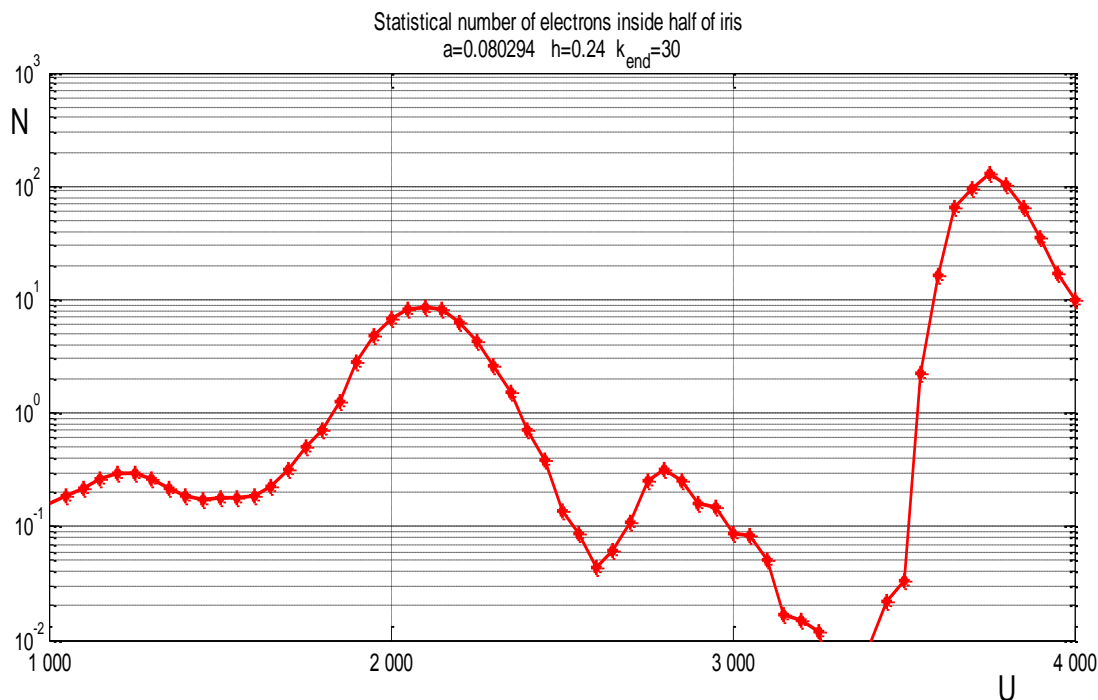


Fig. 6. The relative number of electrons after 15 microwave periods inside half iris structure with height 0.12 cm and length 0.08 cm

The software MULSIM makes it possible to predict the multipactor threshold in microwave structures with half irises. This software also makes it possible to simulate the multipactor avalanche in arbitrary rectangular structures taking into account a spread of electron initial velocities, the action of the microwave magnetic field on the electron motion, and measured data of the dependence of the secondary emission yield on electron impact energy. It should also be noted that the software allow users to vary the position of seed electrons, to choose different probability distributions for the initial velocities of secondary electrons, and to compute as many electron trajectories as necessary in order to avoid stochastic fluctuations and thereby obtain reliable predictions of the multipactor threshold.

#### 4. CORONA EFFECT AT ATMOSPHERIC PRESSURE

In the Corona domain, an analysis of a simplified model has been made to understand Corona breakdown due to gas heating at atmospheric pressure. An investigation of the thermal stability properties of a breakdown plasma situated in a homogeneous electric RF field in a gas where electron losses are governed mainly by the attachment process has been performed. This study demonstrated that when the original size of the region of gas heating exceeds some threshold value the breakdown inside this region initiates unlimited expansion of the discharge even if the field amplitude is below the breakdown threshold in cold gas.